



## Ultra-low power all-optical wavelength conversion of high-speed data signals in high-confinement AlGaAs-on-insulator microresonators

Stassen, Erik; Kim, Chanju; Kong, Deming; Hu, Hao; Galili, Michael; Oxenløwe, Leif Katsuo; Yvind, Kresten; Pu, Minhao

*Published in:*  
APL Photonics

*Link to article, DOI:*  
[10.1063/1.5115232](https://doi.org/10.1063/1.5115232)

*Publication date:*  
2019

*Document Version*  
Publisher's PDF, also known as Version of record

[Link back to DTU Orbit](#)

### *Citation (APA):*

Stassen, E., Kim, C., Kong, D., Hu, H., Galili, M., Oxenløwe, L. K., Yvind, K., & Pu, M. (2019). Ultra-low power all-optical wavelength conversion of high-speed data signals in high-confinement AlGaAs-on-insulator microresonators. *APL Photonics*, 4(10), [100804]. <https://doi.org/10.1063/1.5115232>

---

### General rights

Copyright and moral rights for the publications made accessible in the public portal are retained by the authors and/or other copyright owners and it is a condition of accessing publications that users recognise and abide by the legal requirements associated with these rights.



- Users may download and print one copy of any publication from the public portal for the purpose of private study or research.
- You may not further distribute the material or use it for any profit-making activity or commercial gain
- You may freely distribute the URL identifying the publication in the public portal

If you believe that this document breaches copyright please contact us providing details, and we will remove access to the work immediately and investigate your claim.

# Ultra-low power all-optical wavelength conversion of high-speed data signals in high-confinement AlGaAs-on-insulator microresonators F

Cite as: APL Photonics 4, 100804 (2019); <https://doi.org/10.1063/1.5115232>

Submitted: 15 June 2019 . Accepted: 16 September 2019 . Published Online: 09 October 2019

Erik Stassen, Chanju Kim (김찬주), Deming Kong (孔德明), Hao Hu (胡浩), Michael Galili, Leif Katsuo Oxenløwe, Kresten Yvind , and Minhao Pu (蒲敏皓) 

## COLLECTIONS

Note: This article is part of the Special Topic on Hybrid Integration beyond Silicon Photonics.

F This paper was selected as Featured



View Online



Export Citation



CrossMark

additive manufacturing epitaxial crystal growth cerium oxide polishing powder silver nanoparticles sputtering targets III-IV semiconductors CVD precursors europium phosphors



**AMERICAN ELEMENTS**

THE ADVANCED MATERIALS MANUFACTURER®

deposition slugs LEDs lighting spintronics solar energy osmium nanoribbons thin films chalcogenides AuNP

GDC Li-ion battery electrolytes 99.999% ruthenium spheres endohedral fullerenes copper nanoparticles diamond micropowder CIGS MBE grade materials palladium catalysts flexible electronics beta-barium borate borosilicate glass dysprosium pellets YBCO pyrolytic graphite 3D graphene foam iodine tin oxide mesoporous silica saron substrates sapphire windows tungsten carbide InGaAs barium fluoride carbon nanotubes lithium niobate scandium powder



gallium lamp glassy carbon nanodispersions InAs wafers laser crystals ultra high purity materials MOCs rare earth metals photovoltaics refractory metals MOCVD superconductors transparent ceramics ultra high purity silicon

*American Elements opens up a world of possibilities so you can **Now Invent!***

Over 15,000 certified high purity laboratory chemicals, metals, & advanced materials and a state-of-the-art Research Center. Printable GHS-compliant Safety Data Sheets. Thousands of new products. And much more. All on a secure multi language "Mobile Responsive" platform.

perovskite crystals yttrium iron garnet alternative energy Li-Ion gold nanocubes graphene oxide macromolecules photonics rhodium sponge fiber optics beamsplitters infrared dyes zeolites fused quartz metallocenes platinum ink buckyballs Ti-6Al-4V

**Now Invent.™**  
The Next Generation of Material Science Catalogs

[www.americanelements.com](http://www.americanelements.com)



# Ultra-low power all-optical wavelength conversion of high-speed data signals in high-confinement AlGaAs-on-insulator microresonators



Cite as: APL Photon. 4, 100804 (2019); doi: 10.1063/1.5115232

Submitted: 15 June 2019 • Accepted: 16 September 2019 •

Published Online: 9 October 2019



Erik Stassen, Chanju Kim (김찬주), Deming Kong (孔德明), Hao Hu (胡浩), Michael Galili, Leif Katsuo Oxenløwe, Kresten Yvind,<sup>a)</sup> and Minhao Pu (蒲敏皓)<sup>a)</sup>

## AFFILIATIONS

DTU Fotonik, Technical University of Denmark, Ørstedes Plads 343, 2800 Kgs. Lyngby, Denmark

**Note:** This article is part of the Special Topic on Hybrid Integration beyond Silicon Photonics.

<sup>a)</sup>Electronic addresses: kryv@fotonik.dtu.dk and mipu@fotonik.dtu.dk.

## ABSTRACT

Wavelength conversion technology is imperative for the future high-speed all-optical network. Nonlinear four-wave mixing (FWM) has been used to demonstrate such functionality in various integrated platforms because of their potential for the realization of a chip-scale, fully integrated wavelength converter. Until now, waveguide-based wavelength conversion on a chip requires a pump power beyond the reach of available on-chip lasers. Although high-quality factor ( $Q$ ) microresonators can be utilized to enhance the FWM efficiency, their narrow resonance linewidths severely limit the maximal data rate in wavelength conversion. In this work, combining the ultrahigh effective nonlinearity from a high-confinement aluminum gallium arsenide waveguide and field enhancement from a microring resonator with a broad resonance linewidth, we realize all-optical wavelength conversion of a 10-Gbaud data signal by using a pump power, for the first time, at a submilliwatt level. With such a low operation power requirement, a fully integrated high-speed wavelength converter is envisioned for the future all-optical network. The waveguide cross-sectional dimension is engineered in a submicron scale to enhance the light confinement, which pushes the device effective nonlinearity to  $720 \text{ W}^{-1} \text{ m}^{-1}$  while maintaining a broad operation bandwidth covering the telecom S-, C-, and L-bands. Moreover, we demonstrate that a single microring resonator is capable of handling a high-speed data signal at a baud rate up to 40 Gbit/s. All the wavelength conversion experiments are validated with bit-error rate measurements.

© 2019 Author(s). All article content, except where otherwise noted, is licensed under a Creative Commons Attribution (CC BY) license (<http://creativecommons.org/licenses/by/4.0/>). <https://doi.org/10.1063/1.5115232>

Optical signal processing (OSP) has the potential to vastly outperform its electrical counterpart in terms of both capacity and power consumption.<sup>1</sup> A critical operation within OSP is optical routing,<sup>2</sup> which can be realized by wavelength conversion through the parametric four-wave mixing (FWM) process.<sup>3</sup> The FWM-based wavelength conversion offers strict transparency with respect to modulation formats by preserving phase and amplitude information and may play a key role in interconnecting wavelength division multiplexing (WDM) networks.

In recent years, integrated photonic chips have been shown to be able to perform highly efficient FWM. The dispersion engineering

enables ultrabroadband operation in integrated waveguides, and the femtosecond-scale response of the parametric FWM process enables ultrafast OSP.<sup>4</sup> The development of heterogeneous integration technology<sup>5</sup> makes it possible to combine laser and nonlinear materials on a single complementary metal-oxide-semiconductor (CMOS)-compatible chip realizing on-chip laser-driven wavelength converters. However, most of the integrated waveguide-based wavelength conversion demonstrations<sup>6–16</sup> require a pump power beyond the reach of available on-chip lasers.

Microresonators can be utilized to enhance the FWM efficiency significantly because of the large circulating power.<sup>17,18</sup> Efforts on

pushing the quality factor ( $Q$ ) for such integrated nonlinear microresonators have led to optical parametric oscillation and thus frequency comb generation.<sup>19</sup> However, for high-speed OSP, the narrow resonance linewidth (in the order of megahertz) of such high  $Q$  microresonators limits the maximal data rate, as the optical response of the resonance is essentially a bandpass filter. Therefore, the benefit of efficiency enhancement in microresonators is severely constrained in OSP of the high-speed data signal (at the gigahertz data modulation speed). Because of this, there are only a few demonstrations for OSP of data signals in microresonators so far<sup>20–23</sup> although the prospect of wavelength conversion in microring resonators has been suggested two decades ago.<sup>17</sup> In low-index material platforms such as Hydex, wavelength conversion of a data signal at a speed of 2.5 Gbit/s has been demonstrated in a microring resonator.<sup>20</sup> Because of the low device nonlinearity, the required pump power is larger than 150 mW. In the case of high-index material platforms such as silicon, Hu *et al.* demonstrated a wavelength conversion of a 10 Gbit/s quadrature phase shift keying data signal in a microring resonator with a graphene layer deposited on top. Although the required pump was reduced to 20 mW because of a higher device nonlinearity, the conversion efficiency is limited due to the two-photon absorption (TPA) in silicon and high absorption loss of graphene.<sup>21</sup> Therefore, an integrated platform with high device nonlinearity and low nonlinear loss is highly desirable to take advantages of the efficiency enhancement from microresonators in wavelength conversion of high-speed data signals. It is worth noting that although the signal wave will experience a phase change at a resonance, the original phase information can be recovered by using phase recovery algorithms [e.g., decision-directed phase-locked loop (DDPLL) and blind phase search] in the digital signal processing (DSP) flow in the coherent detection because the phase response for a certain microresonator is fixed and known. Therefore, microresonators are also suitable for FWM-based wavelength conversion for advanced modulation formats such as quadrature amplitude modulation (QAM).

In the last decade, tremendous efforts have been made to develop different integrated nonlinear material platforms.<sup>16–34</sup> Among those platforms, our recently developed platform AlGaAs-on-insulator (AlGaAsOI)<sup>29</sup> exhibits an ultrahigh effective nonlinear coefficient as an AlGaAsOI nanowaveguide combines a large material nonlinear index (on the order of  $10^{-17}$  W/m<sup>2</sup>) and strong light confinement due to its high index contrast. The bandgap of AlGaAs can be engineered to mitigate TPA at telecommunication wavelengths.<sup>35</sup> Thanks to the ultrahigh effective nonlinearity, we have previously demonstrated OSP at speeds beyond Terabit per second by ultrabroadband wavelength conversion,<sup>36</sup> wavelength conversion of 256-QAM data signals,<sup>37</sup> and a broadband frequency comb source supporting 661 Tbit/s data transmission<sup>38</sup> based on dispersion engineered AlGaAsOI nanowaveguides. In this work, we reduce the waveguide cross-sectional dimension compared to our earlier work ( $280\text{ nm} \times 640\text{ nm}$ )<sup>36</sup> to enhance the effective nonlinear coefficient to  $720\text{ W}^{-1}\text{ m}^{-1}$ . The waveguide dispersion is kept low enough to ensure a broad FWM bandwidth over 130 nm. We fabricate AlGaAsOI microresonators with such a waveguide dimension that they exhibit moderate Qs (resonance linewidths at a gigahertz range). We achieve ultraefficient continuous-wave (CW) FWM processes in the microring resonators and realize a wavelength conversion of 10-Gbaud non-return-zero on-off-key (NRZ-OOK) data signal using a pump power of just 0.9 mW. We evaluate the influence of

the filtering effect, induced by the finite resonance linewidth, on high-speed wavelength conversion in a single microresonator by pushing the operating data rate to 40 Gbit/s. Such highly nonlinear microresonators can be a building block for next-generation WDM network.

The schematic illustration of FWM-based all-optical wavelength conversion in a nonlinear microring resonator is shown in Fig. 1(a). The low-power CW pumping light (green) and the data encoded light pulses (blue) are evanescently coupled from the bus waveguide to the microring resonator. Circulating in the nonlinear resonator, both pump and signal power build up to such a high level that an FWM process results in an efficient generation of idler pulses at another frequency (red) and thus replication of data signals from one frequency to another at the output of the photonic AlGaAsOI chip. The AlGaAsOI wafer, where a high-quality thin AlGaAs film on top of a low-index insulator layer (SiO<sub>2</sub>) resides on a semiconductor substrate, is fabricated through wafer bonding and substrate removal processes.<sup>39</sup> The AlGaAsOI microring resonators are defined using an optimized electron-beam lithography process<sup>40</sup> and a chloride-based dry etching process. Figure 1(b) shows the scanning electron microscopy (SEM) image of a fabricated AlGaAsOI microresonator with a diameter of  $34.4\text{ }\mu\text{m}$  and a free spectral range (FSR) of 690 GHz. Figure 1(c) shows the AlGaAsOI waveguide with a nominal cross-sectional dimension of  $290\text{ nm} \times 465\text{ nm}$ . Such submicron dimensions offer an ultrahigh effective nonlinearity of  $720\text{ W}^{-1}\text{ m}^{-1}$  (see the supplementary material), which is larger than our previous result<sup>29</sup> due to the reduced effective mode area. According to our previous characterization of AlGaAsOI waveguides,<sup>39</sup> the propagation loss will increase from 1.3 dB/cm to around 2 dB/cm when the waveguide width is reduced from 640 nm to around 465 nm. To prepare the AlGaAsOI chip for characterization, inverted-nano tapers<sup>41</sup> were used at both sample facets to facilitate an efficient fiber-to-chip coupling (3 dB/facet).

The experimental setup for the wavelength conversion of the NRZ-OOK data signal is shown in Fig. 1(d). In the transmitter, a CW light emitted from an external-cavity laser is modulated by a modulator to generate a high-speed (10–40 Gbit/s) NRZ-OOK data signal. The generated signal pulses at 1538.2 nm are coupled into the photonic chip-based wavelength converter where CW light at 1543.6 nm is used as the pump wave. Both pump and signal waves are aligned to the TE polarization of the AlGaAsOI nanowaveguide while their wavelengths are tuned to the resonant wavelengths of the AlGaAsOI microresonator. Erbium-doped fiber amplifiers (EDFAs) are used to adjust the coupled power for both pump and signal waves. Bandpass filters (BPFs) are used before and after the AlGaAsOI chip to filter out the amplified spontaneous emission (ASE) noise from the EDFAs and to separate the pump and signal waves at the output. The converted idler is then sent to the receiver where the idler is evaluated by a bit-error-rate tester (BERT).

We first performed wavelength conversion of a 10-Gbit/s data signal in an AlGaAsOI microring resonator where there is little filtering penalty induced by the resonance linewidth. An overcoupled microring resonator with a resonance linewidth of  $\sim 10$  GHz was used in this case (see the supplementary material). In the experiment, the pump laser was first manually tuned following the resonance thermal red-shift until thermal soft locking is achieved<sup>42</sup> where the heating of the resonator was balanced by convective and diffusive cooling. As the average power of the signal pulses was

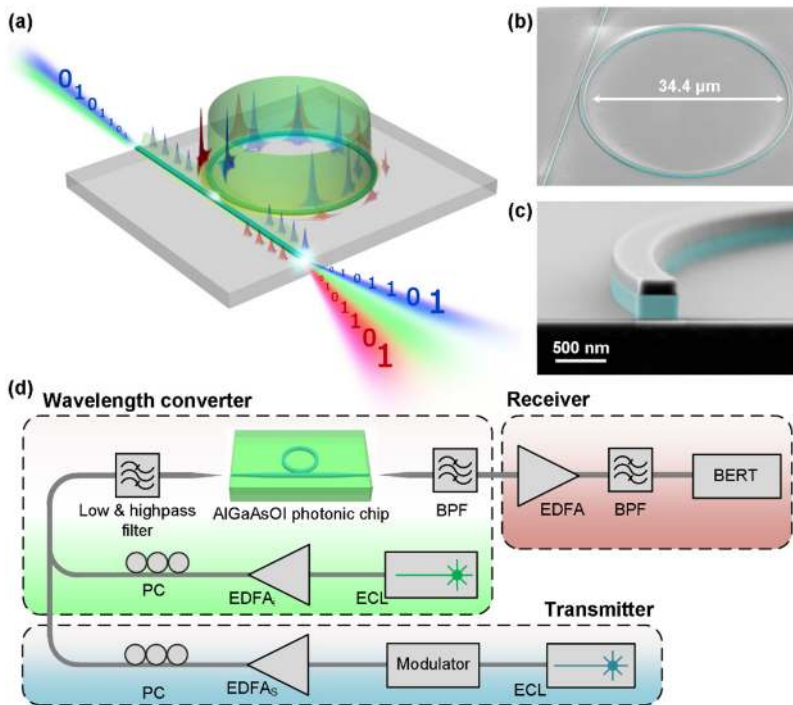


**FIG. 1.** (a) Schematic illustration of all-optical wavelength conversion of data signals based on four-wave mixing (FWM) in a nonlinear microring resonator on an AlGaAs-on-insulator (AlGaAsOI) chip. [(b) and (c)] Scanning electron microscopy (SEM) pictures of an AlGaAsOI microring resonator with a diameter of  $34.4\ \mu\text{m}$  (b) and the cross section of its waveguide (c) before it is clad with a silica layer. The AlGaAs material is denoted by artificial blue color, and the top left-over layer is the electron-beam resist which is used as an etching mask for patterning. (d) Experimental setup for all-optical wavelength conversion of a high-speed data signal using a nonlinear AlGaAsOI chip.

always kept 6-dB lower than that of the CW pump light, after the signal laser was tuned into the resonance, only a few iterative fine-tuning operations were performed for the pump and signal wavelengths to achieve the maximum conversion efficiency. Although no temperature controlling element is used during the bit-error rate (BER) characterization, the power variation of the converted signal is kept less than 1 dB, thanks to the relatively large resonance linewidth. With a coupled pump power of 2.9 mW, the measured BER of the back-to-back signal (blue) and wavelength converted idler (red) are shown in Fig. 2(b), where an error-free operation (BER =  $10^{-9}$ ) was achieved for the idler with a conversion efficiency of  $-21.6$  dB (see the supplementary material). Figure 2(c) shows the measured BER and conversion efficiency as a function of the coupled pump power in the bus waveguide. It is seen that the achieved BER is below the hard-decision forward error correction (HD-FEC) threshold ( $3.8 \times 10^{-3}$  with 7% overhead), which is required to perform FEC on the converted idler data signal to get error-free operation (BER <  $10^{-12}$ ). The pump power is only 0.9 mW, which corresponds to a very low switching energy per bit (90 fJ/bit).

To realize such a submilliwatt power operation, we engineered the AlGaAsOI nanowaveguide in such a way that the device effective nonlinearity can be enhanced while the dispersion is maintained low enough to support a broadband operation in the commonly used telecommunication bands. To perform FWM characterization without a data signal, we use the setup shown in Fig. 1(d) with the modulator by-passed and the receiver replaced by an optical spectrum analyzer (OSA). Figure 2(d) shows the measured normalized conversion efficiency of the microring resonator and the waveguide as a function of signal wavelength. The simulated conversion efficiency matches well with the measured data for the 3-mm-long

waveguide and shows a 3-dB bandwidth of about 130 nm covering the telecom S-, C-, and L-bands. We obtained nearly constant conversion efficiency within the entire tuning range of our signal laser source although some efficiency fluctuation can be found due to the variation of  $Q$  over the different resonances.

The FWM efficiency can be further enhanced to reduce the required pump power if the signal to be converted is with a lower data rate. We measured the FWM conversion efficiency for microresonators with the same intrinsic  $Q$  ( $\sim 10^5$ ) but with different coupling conditions (coupling gaps: 210–330 nm) when the pump power is fixed at 1 mW. The conversion efficiency is defined by the ratio between the generated idler power and the coupled signal power (see the supplementary material). As shown in Fig. 2(e), one can find the trade-off between the achievable conversion efficiency and the maximal data rate the device can handle without a filtering effect.<sup>43</sup> The efficiency reaches the maximum at a slightly undercoupled condition (linewidth of 2.6 GHz), and the achievable data rate reaches the maximum at a very overcoupled condition (linewidth of 9.7 GHz). Figure 2(f) shows the measured normalized transmission spectra in these two cases. As the coupling coefficient between the bus and the ring is a determining factor in the resonance linewidth and the conversion efficiency, active tuning of the coupling region<sup>44</sup> could be a practical scheme for optimizing the device performance on-the-fly. In the case where a high data rate is crucial, one may use the device with a broad resonance linewidth at the expense of a compromised efficiency.

The resonance linewidth limits the maximal data rate for the wavelength conversion as the filtering effects lead to spectral distortion and sideband attenuation. To support wavelength conversion at a higher data rate beyond 10 Gbit/s, we used a microresonator with

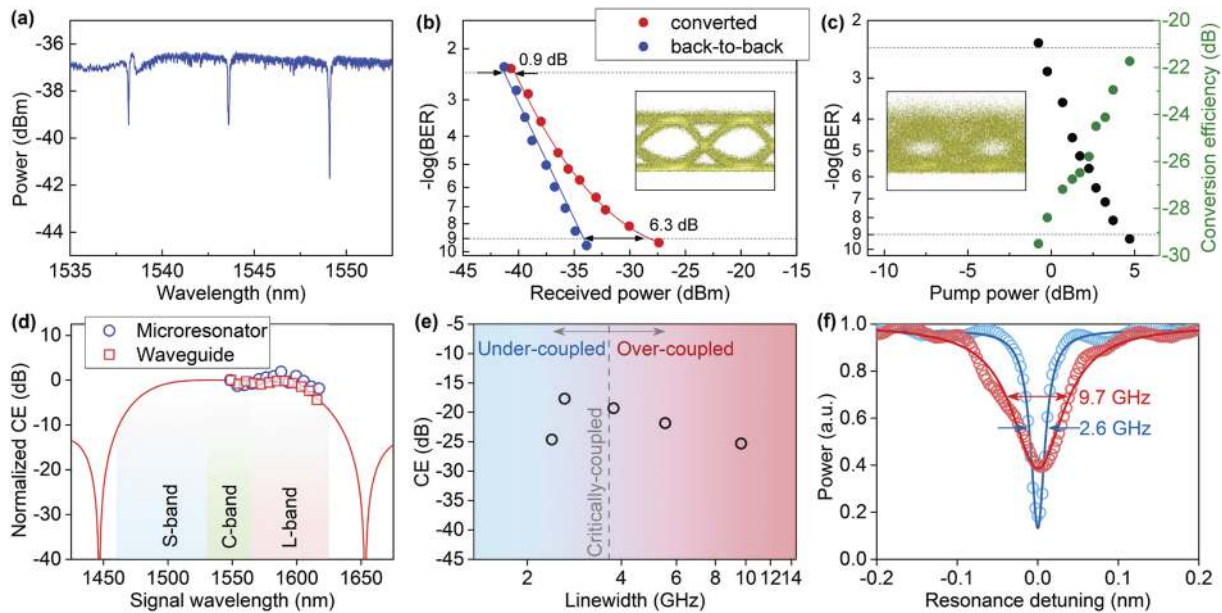


**FIG. 2.** (a) Measured transmission spectrum of an overcoupled AlGaAsOI microresonator with an intrinsic Q factor of around  $10^5$  and a resonance linewidth of around 10 GHz. (b) Bit-error rate (BER) measurements for the 10 Gbit/s back-to-back and wavelength converted signal from the AlGaAsOI microring resonator vs the received power with system penalties indicated at BER =  $3.8 \times 10^{-3}$  (hard-FEC limit) and BER =  $1 \times 10^{-9}$  (error-free limit), respectively. The inset shows the eye diagrams with BER error-free limit. (c) Measured BER (black) and conversion efficiency (CE) (green) for 10 Gbit/s wavelength conversion vs the total coupled power in the bus waveguide. The inset shows the eye diagrams at the HD-FEC limit. (d) Measured normalized CE vs signal wavelength. (e) CE vs resonance linewidth at a pump power of 1 mW. Different coupling conditions are indicated as blue (undercoupled), gray dashed line (critically coupled), and red (overcoupled). (f) Measured normalized transmission spectra of the microresonators with different coupling gaps (blue: 300 nm, red: 210 nm). The colored circles are the measured data, and the colored solid curves are the corresponding fit (Lorentzian); the colored arrows indicate the corresponding linewidth of the resonances.

a lower intrinsic Q ( $\sim 2.7 \times 10^4$ ) than those used in the aforementioned experiment. Operated in a highly overcoupled condition, the microring resonator has a resonance linewidth of about 25 GHz (see the [supplementary material](#)). In the wavelength conversion experiment, a fixed pump power of 32 mW was used to achieve a conversion efficiency of approximately -16 dB. In order to test the data rate limit and the influence of the filtering effect when the signal pulses have a spectral bandwidth larger than the resonance linewidth of the resonator, we also increased the data rate from 30 Gbit/s to 40 Gbit/s for the signal pulses.

Figure 3(a) shows the measured BER for the wavelength conversion of the 30-Gbit/s data signal. The system penalty is indicated by the horizontal arrows. Even with the presence of the detrimental filtering effect, it is still possible to achieve error-free operation (with BER at  $10^{-9}$ ) due to the high conversion efficiency. Figure 3(b) shows the BER measurement in the case of a data signal at a speed of 40 Gbit/s. Although an error floor is observed due to the strong filtering effects, we obtained a BER below the hard-FEC limit ( $3.8 \times 10^{-3}$ ) with a system penalty of 8.8 dB. We measured the system penalty at the hard-FEC limit as a function of the data rates from

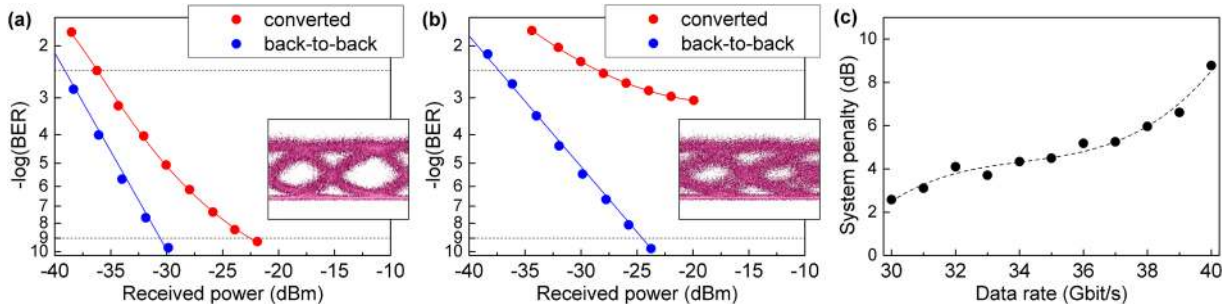


**FIG. 3.** (a) Measured BER for the 30 Gbit/s back-to-back and wavelength converted data signal. Inset: eye diagram of the wavelength converted signal at BER =  $10^{-9}$ . (b) Measured BER for the 40 Gbit/s back-to-back and wavelength converted data signal. Inset: eye diagram of the wavelength converted signal at BER =  $3.8 \times 10^{-3}$ . (c) Measured system penalty as a function of the data rate with BER at the HD-FEC limit.

30 Gbit/s to 40 Gbit/s, as shown in Fig. 3(c), where a steady increase in penalty for higher data rates due to the filtering effect is evident. Data rates below 30 Gbit/s were not measured, as it is expected that due to a small filtering effect, the system penalty would be much smaller. Because of the reduced build-up factor in the microring resonator with a relatively larger resonance linewidth, the required pump power is increased by more than an order of magnitude compared with the 10-Gbit/s wavelength conversion case.

Table I shows a performance comparison of different approaches (waveguide designs and nonlinear materials) in FWM-based wavelength conversion. Most of the wavelength conversion demonstrations are realized in strip or slab waveguides.<sup>9–12,29</sup> Efforts to enhance the light confinement enabled efficient FWM in short waveguides while dispersion engineering enabled ultrabroadband operation. It allows wavelength conversion of data signals at a record-high speed (>600 Gbit/s).<sup>10,29</sup> However, the required pump power level is still at the few-tenth-milliwatt level. To further enhance the effective nonlinearity, slow-light effects in photonic crystal (PhC) waveguides have been exploited. As the effective nonlinearity scales as the square of the slowdown factor, up to  $2900 \text{ W}^{-1} \text{ m}^{-1}$ , nonlinearity has been demonstrated in a PhC waveguide.<sup>14</sup> However, the major limitation of PhC waveguides is the operation bandwidth of the slow light. State-of-the-art dispersion engineered PhC waveguides exhibit a constant group index of  $\sim 30$  over a 13 nm bandwidth,<sup>45</sup> which results in an even smaller FWM bandwidth and limits their application in OSP. In order to avoid TPA at the telecom wavelengths, different high-index materials such as amorphous silicon (a-Si),<sup>11</sup> chalcogenide,<sup>12</sup> and GaInP<sup>14</sup> have been used as nonlinear materials. Alternatively, low-index nonlinear polymer materials<sup>15,16</sup> have also been used in the silicon slot or plasmonic waveguides. Although a large peak power (>1 W) can be used without suffering from TPA in both cases, no superior FWM performance concerning conversion efficiency and conversion bandwidth is demonstrated due to a relatively low nonlinearity and a large propagation loss for the slot and plasmonic waveguides, respectively. Compared with the aforementioned

approaches, the microresonator-based approach offers more than one order of magnitude lower power consumption and a much smaller device form factor. Combining the ultrahigh effective nonlinearity of AlGaAs and the microresonator design, the required pump power for 10-Gbit/s wavelength conversion can be pushed down to the submilliwatt level while a broad conversion bandwidth (covering S-, C-, and L-bands) is maintained. Although the maximal data rate is not limited by the conversion bandwidth as in PhC waveguides, it is limited by the resonance linewidth in the single-microresonator configuration. The achievable data rate for the wavelength conversion can be increased by using the coupled-resonator optical waveguide (CROW) design.<sup>23</sup> For instance, the overall resonance linewidth of an eight-ring CROW can be increased from 30 GHz to 80 GHz at the expense of a reduced FWM enhancement. Although the CROW is also potentially capable of supporting even higher data rates by a more sophisticated design, the further reduced efficiency enhancement will make the CROW solution less favorable. The advantage of using microresonators (or CROW) still lies in OSP of data signals at a relatively low speed where the operation power can be reduced to within the reach of on-chip laser sources. The CROW design can also be utilized to enhance efficiency.<sup>23</sup> Alternatively, graphene-based materials (e.g., graphene oxide<sup>46</sup>) with a giant Kerr response and a low TPA can be combined with AlGaAsOI devices.

In conclusion, we demonstrate the first submilliwatt pump power wavelength conversion of a high-speed (10 Gbit/s) data signal in an integrated AlGaAsOI microring resonator. The first wavelength conversion in integrated microresonators at data rates beyond 10 Gbit/s, specifically obtaining error-free performance at 30 Gbit/s and the BER remaining below the HD-FEC limit at 40 Gbit/s, has been demonstrated. Despite the inevitable performance trade-off between efficiency enhancement and achievable operating data rate in nonlinear microresonators, the achieved ultrahigh effective nonlinearity and broadband operation make AlGaAsOI the most promising nonlinear platform to realize low-power fully integrated OSP functionality for practical WDM network.

TABLE I. Comparison of different approaches for FWM-based wavelength conversion.

| Device design   | Nonlinear media                | Length | Peak pump power | Conversion efficiency (dB) | Conversion bandwidth (nm) | Idler baud rate | Publication year | References |
|-----------------|--------------------------------|--------|-----------------|----------------------------|---------------------------|-----------------|------------------|------------|
| Strip WG        | Silicon                        | 2.8 cm | 160 mW          | -10.6                      | 19                        | 10 Gbit/s       | 2006             | 9          |
| Strip WG        | Silicon                        | 3 mm   | 71 mW           | -29                        | 140                       | 640 Gbit/s      | 2011             | 10         |
| Strip WG        | a-Si                           | 1.7 cm | 150 mW          | -33                        | 25                        | 10 Gbit/s       | 2012             | 11         |
| Strip WG        | AlGaAs                         | 3 mm   | 35.5 mW         | -23                        | 750                       | 1.28 Tbit/s     | 2018             | 29         |
| Rib WG          | As <sub>2</sub> S <sub>3</sub> | 6 cm   | 730 mW          | -27.5                      | 40                        | 40 Gbit/s       | 2009             | 12         |
| PhC WG          | Silicon                        | 96 μm  | 895 mW          | -33                        | <13                       | 10 Gbit/s       | 2011             | 13         |
| PhC WG          | GaInP                          | 1.5 mm | 100 mW          | -35                        | 8                         | 660 Mbit/s      | 2011             | 14         |
| Slot WG         | Polymer                        | 4 mm   | 1.34 W          | -37                        | 18                        | 42.7 Gbit/s     | 2009             | 15         |
| Plasmonic WG    | Polymer                        | 2 μm   | 30 W            | -13.3                      | 60                        | NA              | 2017             | 16         |
| Microresonator  | Hydex                          | 300 μm | 165 mW          | -28.5                      | 27                        | 2.5 Gbit/s      | 2010             | 20         |
| Microresonator  | Si/Graphene                    | 63 μm  | 20 mW           | -38                        | 20                        | 10 Gbit/s       | 2016             | 21         |
| Microresonators | Silicon                        | 630 μm | 16 mW           | -36                        | 120                       | 10 Gbit/s       | 2011             | 23         |
| Microresonator  | AlGaAs                         | 110 μm | 900 μW          | -28.4                      | 130                       | 10 Gbit/s       | 2019             | This work  |
| Microresonator  | AlGaAs                         | 110 μm | 32 mW           | -16                        | 130                       | 40 Gbit/s       | 2019             | This work  |

See the [supplementary material](#) for device fabrication, nonlinear characterization of AlGaAsOI waveguide, and linear characterization of AlGaAsOI microresonators.

We would like to acknowledge the support from Danmarks Grundforskningsfond Center of Excellence SPOC (Grant No. DNR123) and Villum Young Investigator program (Grant No. 2MAC).

## REFERENCES

- <sup>1</sup>D. Cotter *et al.*, “Nonlinear optics for high-speed digital information processing,” *Science* **286**(5444), 1523–1528 (1999).
- <sup>2</sup>S. J. B. Yoo, “Wavelength conversion technologies for WDM network applications,” *J. Lightwave Technol.* **14**(6), 955–966 (1996).
- <sup>3</sup>J. Leuthold, C. Koos, and W. Freude, “Nonlinear silicon photonics,” *Nat. Photonics* **4**(8), 535–544 (2010).
- <sup>4</sup>L. K. Oxenlowe *et al.*, “Silicon photonics for signal processing of Tbit/s serial data signals,” *IEEE J. Sel. Top. Quantum Electron.* **18**(2), 996–1005 (2012).
- <sup>5</sup>D. Liang and J. E. Bowers, “Recent progress in lasers on silicon,” *Nat. Photonics* **4**(8), 511–517 (2010).
- <sup>6</sup>M. Pu *et al.*, “Polarization insensitive wavelength conversion in a dispersion-engineered silicon waveguide,” *Opt. Express* **20**(15), 16374 (2012).
- <sup>7</sup>I. Sackey *et al.*, “1.024 Tb/s wavelength conversion in a silicon waveguide with reverse-biased p-i-n junction,” *Opt. Express* **25**(18), 21229 (2017).
- <sup>8</sup>C. J. Krüchel *et al.*, “Continuous wave-pumped wavelength conversion in low-loss silicon nitride waveguides,” *Opt. Lett.* **40**(6), 875 (2015).
- <sup>9</sup>K. Yamada, H. Fukuda, T. Tsuchizawa, T. Watanabe, T. Shoji, and S. Itabashi, “All-optical efficient wavelength conversion using silicon photonic wire waveguide,” *IEEE Photonics Technol. Lett.* **18**(9), 1046–1048 (2006).
- <sup>10</sup>H. Hu *et al.*, “Ultra-high-speed wavelength conversion in a silicon photonic chip,” *Opt. Express* **19**(21), 19886 (2011).
- <sup>11</sup>S. Suda *et al.*, “Pattern-effect-free all-optical wavelength conversion using a hydrogenated amorphous silicon waveguide with ultra-fast carrier decay,” *Opt. Lett.* **37**(8), 1382 (2012).
- <sup>12</sup>F. Luan *et al.*, “Dispersion engineered As<sub>2</sub>S<sub>3</sub> planar waveguides for broadband four-wave mixing based wavelength conversion of 40 Gb/s signals,” *Opt. Express* **17**(5), 3514 (2009).
- <sup>13</sup>B. Corcoran *et al.*, “Ultracompact 160 Gbaud all-optical demultiplexing exploiting slow light in an engineered silicon photonic crystal waveguide,” *Opt. Lett.* **36**(9), 1728 (2011).
- <sup>14</sup>I. Cestier *et al.*, “Time domain switching/demultiplexing using four wave mixing in GaInP photonic crystal waveguides,” *Opt. Express* **19**(7), 6093 (2011).
- <sup>15</sup>T. Vallaitis *et al.*, “All-optical wavelength conversion at 42.7 Gbit/s in a 4 mm long silicon-organic hybrid waveguide,” in *Optical Fiber Communication Conference and National Fiber Optic Engineers Conference* (Optical Society of America, 2009), p. OWS3.
- <sup>16</sup>M. P. Nielsen, X. Shi, P. Dichtl, S. A. Maier, and R. F. Oulton, “Giant nonlinear response at a plasmonic nanofocus drives efficient four-wave mixing,” *Science* **358**(6367), 1179–1181 (2017).
- <sup>17</sup>P. P. Absil *et al.*, “Wavelength conversion in GaAs micro-ring resonators,” *Opt. Lett.* **25**(8), 554 (2000).
- <sup>18</sup>M. Ferrera *et al.*, “Low power four wave mixing in an integrated, micro-ring resonator with Q = 12 million,” *Opt. Express* **17**(16), 14098–14103 (2009).
- <sup>19</sup>D. J. Moss, R. Morandotti, A. L. Gaeta, and M. Lipson, “New CMOS-compatible platforms based on silicon nitride and hydex for nonlinear optics,” *Nat. Photonics* **7**(8), 597–607 (2013).
- <sup>20</sup>A. Pasquazi *et al.*, “All-optical wavelength conversion in an integrated ring resonator,” *Opt. Express* **18**(4), 3858 (2010).
- <sup>21</sup>X. Hu *et al.*, “Graphene-silicon microring resonator enhanced all-optical up and down wavelength conversion of QPSK signal,” *Opt. Express* **24**(7), 7168 (2016).
- <sup>22</sup>C.-L. Wu *et al.*, “Enhancing optical nonlinearity in a nonstoichiometric SiN waveguide for cross-wavelength all-optical data processing,” *ACS Photonics* **2**(8), 1141–1154 (2015).
- <sup>23</sup>F. Morichetti, A. Canciamilla, C. Ferrari, A. Samarelli, M. Sorel, and A. Melloni, “Travelling-wave resonant four-wave mixing breaks the limits of cavity-enhanced all-optical wavelength conversion,” *Nat. Commun.* **2**, 296 (2011).
- <sup>24</sup>B. Kuyken *et al.*, “Nonlinear properties of and nonlinear processing in hydrogenated amorphous silicon waveguides,” *Opt. Express* **19**(26), B146 (2011).
- <sup>25</sup>H. Jung, C. Xiong, K. Y. Fong, X. Zhang, and H. X. Tang, “Optical frequency comb generation from aluminum nitride microring resonator,” *Opt. Lett.* **38**(15), 2810–2813 (2013).
- <sup>26</sup>B. J. M. Hausmann, I. Bulu, V. Venkataraman, P. Deotare, and M. Lončar, “Diamond nonlinear photonics,” *Nat. Photonics* **8**(5), 369–374 (2014).
- <sup>27</sup>C.-L. Wu, Y.-J. Chiu, C.-L. Chen, Y.-Y. Lin, A.-K. Chu, and C.-K. Lee, “Four-wave-mixing in the loss low submicrometer Ta<sub>2</sub>O<sub>5</sub> channel waveguide,” *Opt. Lett.* **40**(9), 4528 (2015).
- <sup>28</sup>U. D. Dave *et al.*, “Nonlinear properties of dispersion engineered InGaP photonic wire waveguides in the telecommunication wavelength range,” *Opt. Express* **23**(4), 4650 (2015).
- <sup>29</sup>M. Pu, L. Ottaviano, E. Semenova, and K. Yvind, “Efficient frequency comb generation in AlGaAs-on-insulator,” *Optica* **3**(8), 823 (2016).
- <sup>30</sup>K. J. A. Ooi *et al.*, “Pushing the limits of CMOS optical parametric amplifiers with USRN:Si<sub>7</sub>N<sub>3</sub> above the two-photon absorption edge,” *Nat. Commun.* **8**, 13878 (2017).
- <sup>31</sup>X. Guan, H. Hu, L. K. Oxenlowe, and L. H. Frandsen, “Compact titanium dioxide waveguides with high nonlinearity at telecommunication wavelengths,” *Opt. Express* **26**(2), 1055 (2018).
- <sup>32</sup>H. El Dirani *et al.*, “Annealing-free Si<sub>3</sub>N<sub>4</sub> frequency combs for monolithic integration with Si photonics,” *Appl. Phys. Lett.* **113**(8), 081102 (2018).
- <sup>33</sup>E. Stassen, M. Pu, E. Semenova, E. Zavarin, W. Lundin, and K. Yvind, “High-confinement gallium nitride-on-sapphire waveguides for integrated nonlinear photonics,” *Opt. Lett.* **44**(5), 1064 (2019).
- <sup>34</sup>Y. Zheng *et al.*, “High-quality factor, high-confinement microring resonators in 4H-silicon carbide-on-insulator,” *Opt. Express* **27**(9), 13053 (2019).
- <sup>35</sup>J. S. S. Aitchison, D. C. C. Hutchings, J. U. U. Kang, G. I. I. Stegeman, and A. Villeneuve, “The nonlinear optical properties of AlGaAs at the half band gap,” *IEEE J. Quantum Electron.* **33**(3), 341–348 (1997).
- <sup>36</sup>M. Pu *et al.*, “Ultra-efficient and broadband nonlinear AlGaAs-on-insulator chip for low-power optical signal processing,” *Laser Photonics Rev.* **12**(12), 1800111 (2018).
- <sup>37</sup>F. Da Ros *et al.*, “Characterization and optimization of a high-efficiency AlGaAs-on-insulator-based wavelength converter for 64- and 256-QAM signals,” *J. Lightwave Technol.* **35**(17), 3750–3757 (2017).
- <sup>38</sup>H. Hu *et al.*, “Single-source chip-based frequency comb enabling extreme parallel data transmission,” *Nat. Photonics* **12**(8), 469–473 (2018).
- <sup>39</sup>L. Ottaviano, M. Pu, E. Semenova, and K. Yvind, “Low-loss high-confinement waveguides and microring resonators in AlGaAs-on-insulator,” *Opt. Lett.* **41**(17), 3996 (2016).
- <sup>40</sup>Y. Zheng, M. Pu, H. K. Sahoo, E. Semenova, and K. Yvind, “High-quality-factor AlGaAs-on-sapphire microring resonators,” *J. Lightwave Technol.* **37**(3), 868–874 (2019).
- <sup>41</sup>M. Pu, L. Liu, H. Ou, K. Yvind, and J. M. Hvam, “Ultra-low-loss inverted taper coupler for silicon-on-insulator ridge waveguide,” *Opt. Commun.* **283**(19), 3678–3682 (2010).
- <sup>42</sup>I. S. Grudin, N. Yu, and L. Maleki, “Generation of optical frequency combs with a CaF<sub>2</sub> resonator,” *Opt. Lett.* **34**(7), 878 (2009).
- <sup>43</sup>B. G. Lee, B. A. Small, K. Bergman, Q. Xu, and M. Lipson, “Transmission of high-data-rate optical signals through a micrometer-scale silicon ring resonator,” *Opt. Lett.* **31**(18), 2701 (2006).
- <sup>44</sup>M. J. Strain, C. Lacava, L. Meriggi, I. Cristiani, and M. Sorel, “Tunable Q-factor silicon microring resonators for ultra-low power parametric processes,” *Opt. Lett.* **40**(7), 1274 (2015).
- <sup>45</sup>J. Li, L. O’Faolain, I. H. Rey, and T. F. Krauss, “Four-wave mixing in photonic crystal waveguides: Slow light enhancement and limitations,” *Opt. Express* **19**(5), 4458 (2011).
- <sup>46</sup>Y. Yang *et al.*, “Enhanced four-wave mixing in waveguides integrated with graphene oxide,” *APL Photonics* **3**(12), 120803 (2018).